AMERICAN SOCIETY FOR MICROBIOLOGY | Antimicrobial Agents and Chemotherapy®

ANTIVIRAL AGENTS

# Efficacy of a Cap-Dependent Endonuclease Inhibitor and Neuraminidase Inhibitors against H7N9 Highly Pathogenic Avian Influenza Virus Causing Severe Viral Pneumonia in Cynomolgus Macaques

**Saori Suzuki,[a] Cong Thanh Nguyen,[a] Ayako Ogata-Nakahara,[a] Akihiro Shibata,[b] Hiroyuki Osaka,[b] Hirohito Ishigaki,[a] Masatoshi Okamatsu,[c] Yoshihiro Sakoda,[c,d] Hiroshi Kida,[d,e,f] Kazumasa Ogasawara,[a] Yasushi Itoh[a]**

[a]Division of Pathogenesis and Disease Regulation, Department of Pathology, Shiga University of Medical Science, Otsu, Shiga, Japan
[b]Exotic Disease Inspection Division, Laboratory Department, Animal Quarantine Service, Ministry of Agriculture, Forestry and Fisheries, Tokoname, Aichi, Japan
[c]Laboratory of Microbiology, Department of Disease Control, Faculty of Veterinary Medicine, Hokkaido University, Sapporo, Hokkaido, Japan
[d]Global Institution for Collaborative Research and Education, Hokkaido University, Sapporo, Hokkaido, Japan
[e]National Research Center for the Control and Prevention of Infectious Diseases, Nagasaki University, Nagasaki, Japan
[f]Research Center for Zoonosis Control, Hokkaido University, Sapporo, Hokkaido, Japan

**ABSTRACT** H7N9 highly pathogenic avian influenza virus (HPAIV) infection in a human was first reported in 2017. A/duck/Japan/AQ-HE29-22/2017 (H7N9) (Dk/HE29-22), found in imported duck meat at an airport in Japan, possesses a hemagglutinin with a multibasic cleavage site, indicating high pathogenicity in chickens, as in the case of other H7 HPAIVs. In the present study, we examined the pathogenicity of Dk/HE29-22 and the effectiveness of a cap-dependent endonuclease inhibitor (baloxavir) and neuraminidase inhibitors (oseltamivir and zanamivir) against infection with this strain in a macaque model ($n = 3$ for each group). All of the macaques infected with Dk/HE29-22 showed severe signs of disease and pneumonia even after the virus had disappeared from lung samples. Virus titers in macaques treated with baloxavir were significantly lower than those in the other treated groups. After infection, levels of interferon alpha and beta (IFN-$\alpha$ and IFN-$\beta$) in the blood of macaques in the baloxavir group were the highest among the groups, whereas levels of tumor necrosis factor alpha (TNF-$\alpha$) and interleukin 13 (IL-13) were slightly increased in the untreated group. In addition, immune checkpoint proteins, including programmed death 1 (PD-1) and T cell immunoreceptor with Ig and ITIM domains (TIGIT), were expressed at high levels in the untreated group, especially in one macaque that showed severe signs of disease, indicating that negative feedback responses against vigorous inflammation may contribute to disease progression. In the group treated with baloxavir, the percentages of PD-1-, CTLA-4-, and TIGIT-positive T lymphocytes were lower than those in the untreated group, indicating that reduction in virus titers may prevent expression of immune checkpoint molecules from downregulation of T cell responses.

**KEYWORDS** H7N9 avian influenza virus, cap-dependent endonuclease inhibitor, highly pathogenic avian influenza virus, immune checkpoint, neuraminidase inhibitor, nonhuman primate

Since 2013, H7N9 low-pathogenic avian influenza viruses (LPAIVs) have been a threat in China, with 1,568 cases of infection and 616 deaths reported up to 2020 (1, 2). In 2016–2017, a period with the largest number of patients infected with H7N9 virus, the emergence of H7N9 highly pathogenic avian influenza viruses (HPAIVs) was first reported in January 2017 (3). H7N9 HPAIVs have caused outbreaks in poultry farms in eight provinces of China. Among the H7N9 HPAIVs, viruses isolated from humans

**Citation** Suzuki S, Nguyen CT, Ogata-Nakahara A, Shibata A, Osaka H, Ishigaki H, Okamatsu M, Sakoda Y, Kida H, Ogasawara K, Itoh Y. 2021. Efficacy of a cap-dependent endonuclease inhibitor and neuraminidase inhibitors against H7N9 highly pathogenic avian influenza virus causing severe viral pneumonia in cynomolgus macaques. Antimicrob Agents Chemother 65:e01825-20. https://doi.org/10.1128/AAC.01825-20.



Address correspondence to Yasushi Itoh, yasushii@belle.shiga-med.ac.jp.

**Received** 23 August 2020
**Returned for modification** 23 September 2020
**Accepted** 18 November 2020
**Accepted manuscript posted online** 30 November 2020
**Published** 17 February 2021

had mutations in the PB2 gene associated with adaptation to mammals (4, 5). In addition, H7N9 HPAIV was isolated from a duck meat product brought to Japan by a flight passenger (6, 7). Therefore, active surveillance of infections with H7N9 HPAIV is necessary to prevent the spread of the virus in poultry and humans.

The virus strain A/duck/Japan/AQ-HE29-22/2017 (H7N9) (Dk/HE29-22) was the first virus isolated outside China from a raw poultry product, which was a combination of skeletal muscle, gizzard, and kidney of a Muscovy duck (*Cairina moschata*) (6). The intravenous pathogenicity index according to the manual of the World Organisation for Animal Health was 2.88 (8), indicating that the virus is highly pathogenic in chickens. Dk/HE29-22 possesses multiple basic amino acid residues, PEVPKRKRTAR/GLF, at the cleavage site in the hemagglutinin (HA) protein, as are found in other HPAIVs (6, 9, 10). In addition, the HA protein of Dk/HE29-22 possesses an L226Q substitution, which is associated with specificity to the avian-type receptor, as well as 186V (H3 numbering), which is associated with binding to the human-type receptor (6, 11, 12). In a previous study using cynomolgus macaques, H7N9 HPAIV (A/Guangdong/17SF003/2016) replicated as efficiently as LPAIV (13), suggesting that Dk/HE29-22 would also replicate effectively in humans.

It is necessary to evaluate the efficacy of antiviral drugs against H7N9 HPAIVs. Neuraminidase inhibitors (NAIs) showed limited effects against H7N9 HPAIV in mice (13), although NAIs were effective against H7N9 LPAIV in a macaque model (14). Therefore, the efficacy of other anti-influenza virus drugs, such as a cap-dependent endonuclease inhibitor (baloxavir), against H7N9 HPAIV needed to be examined in a nonhuman primate model in addition to mouse and ferret models (7, 13, 15, 16).

In the present study, we examined the pathogenicity and efficacy of NAIs and a cap-dependent endonuclease inhibitor against H7N9 HPAIV (Dk/HE29-22), which was isolated from a product collected at an airport in Japan (6). In macaques, Dk/HE29-22 caused severe clinical signs with pneumonia. Macaques treated with NAIs (oseltamivir and zanamivir) and baloxavir showed clinical signs of disease similar to those in the untreated group, but virus titers in the baloxavir group were significantly lower than those in other groups. Therefore, baloxavir was shown for the first time to be effective against H7N9 HPAIV in macaques.

## RESULTS

**Clinical signs of disease and virus propagation in macaques infected with A/duck/Japan/AQ-HE29-22/2017 (H7N9) and effects of antiviral treatments.** We examined the pathogenicity of Dk/HE29-22 isolated from a meat product of a Muscovy duck (*Cairina moschata*) and the efficacy of antiviral drugs in cynomolgus macaques. Body temperatures of all macaques were higher than 39°C within 24 h after virus inoculation and reached temperatures higher than 40°C except for animals W1, W3, and Z1 before treatments (Fig. 1A; also, see Fig. S1 and S2 in the supplemental material). The magnitude of increase in body temperature in the distilled water (DW; control) group was lowest on day 1 after infection (Fig. 1A). However, on the basis of body temperature on day 1 before treatment, body temperatures in the oseltamivir and baloxavir groups showed greater decreases after treatment than those in the DW and zanamivir groups. Average body weights in the DW, zanamivir, and baloxavir groups slightly decreased (Fig. 1C). The clinical scores in all groups increased after virus inoculation due to body temperature increase, nasal discharge, decreased activity, and loss of appetite (Fig. 1C; Table S1). W2 in the control group was euthanized, since the clinical score reached a humane endpoint 3 days after infection. Thus, Dk/HE29-22 caused significant signs of disease in macaques, and antiviral drugs showed no significant effects on the clinical signs. The temperatures, body weights, and clinical signs were not significantly different among the groups.

The virus titers in swab and tissue samples of macaques infected with Dk/HE29-22 were examined. Before the treatments on day 1, the virus was detected in eye, nasal, tracheal, and bronchial swab samples in all groups (Fig. S3A to C; Table 1). The virus was detected in nasal and tracheal samples of the DW group until day 6. On the other

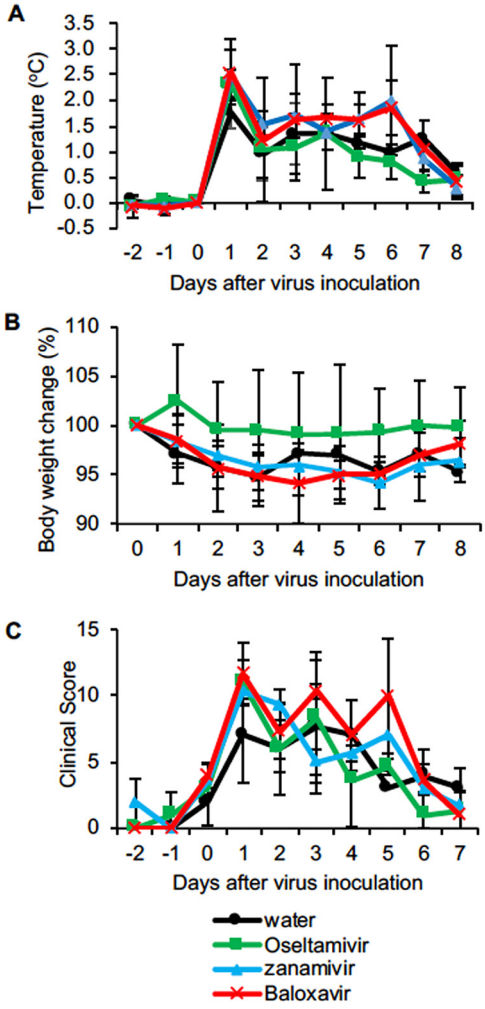


**FIG 1** Clinical signs of disease in macaques infected with H7N9 HPAIV. Cynomolgus macaques ($n = 3$ in each group) were inoculated with the highly pathogenic influenza virus A/duck/Japan/AQ-HE29-22/2017 (H7N9) (Dk/HE29-22). (A) Average body temperatures from 8 p.m. to 8 a.m. the next day were calculated on the basis of data for individual macaques (Fig. S1). Average body temperatures each day were compared with that on day 0 before virus inoculation (Fig. S2). (B) Body weights on indicated days after virus inoculation were compared with that on day 0 before virus inoculation. (C) Clinical scores were determined by daily observation and body temperature according to Table S1. Averages and standard deviations of the results for three monkeys are shown, except for the DW group at 4 to 8 days after virus inoculation, due to the score for W2 reaching the endpoint. No statistically significant differences were found among the groups ($P > 0.05$; Mann-Whitney *U* test).

hand, the virus was detected in nasal samples until day 4, day 5, and day 2 (except for a very low level of virus titer on day 7) in the oseltamivir, zanamivir, and baloxavir groups, respectively, and in tracheal samples until day 5, day 5, and day 2 in the oseltamivir, zanamivir, and baloxavir groups, respectively. The virus was detected in tissues of the nasal mucosa, oronasopharynx, tonsil, trachea, bronchus, lung lobes, and conjunctiva 8 days after infection (Table S2), with high levels in the zanamivir and DW groups. The virus was detected in lung tissues of W2 on day 3. No virus was detected in the pulmonary hilar lymph nodes, hearts, spleens, kidneys, livers, rectum, eyeballs, brain tissues (frontal lobe, temporal lobe, parietal lobe, occipital lobe, cerebellum, brain stem, and olfactory bulb), or muscles in any of the macaques on day 8.

To compare the effects of anti-influenza virus treatments, we calculated the virus titer area under the curve (AUC) after treatment (Fig. S3D to F). The virus titer AUC in bronchial samples of the baloxavir group was significantly lower than those of the oseltamivir and zanamivir groups (Fig. S3F). Thus, baloxavir was more effective than the two NAIs against the H7N9 HPAIV Dk/HE29-22 in macaques.

**TABLE 1** Virus titers in swab samples from cynomolgus macaques infected with Dk/HE29-22

| | | Virus titer ($log_{10}$ $TCID_{50}$/ml) at day after virus inoculation[a] | | | | | | | |
|---|---|---|---|---|---|---|---|---|---|
| Sample | Animal | 1 | 2 | 3 | 4 | 5 | 6 | 7 | 8 |
| Eye swab | W1 | < | < | < | < | < | < | < | < |
| | W2 | 1.77 | < | < | − | − | − | − | − |
| | W3 | 2.67 | 1.50 | 2.00 | < | < | < | < | 0.67 |
| | O1 | 2.33 | < | < | < | < | < | < | < |
| | O2 | < | < | < | < | < | < | < | < |
| | O3 | 2.67 | 1.50 | < | < | < | < | < | < |
| | Z1 | 1.50 | 1.00 | < | < | < | < | < | < |
| | Z2 | 1.67 | < | < | < | < | < | < | < |
| | Z3 | 1.67 | 1.00 | < | < | < | < | < | < |
| | B1 | < | < | < | < | < | < | < | < |
| | B2 | 1.23 | < | < | < | < | < | < | < |
| | B3 | 1.50 | < | < | < | < | < | < | < |
| Nasal swab | W1 | 3.33 | 2.00 | 1.00 | 0.67 | < | < | < | < |
| | W2 | 2.50 | 1.67 | 2.67 | − | − | − | − | − |
| | W3 | 2.33 | 2.67 | 2.33 | < | 1.67 | 1.33 | < | < |
| | O1 | 3.50 | 2.50 | < | 1.23 | < | < | < | < |
| | O2 | 3.50 | 3.00 | 2.17 | < | < | < | < | < |
| | O3 | 2.33 | 2.33 | < | < | < | < | < | < |
| | Z1 | 1.67 | 1.67 | 1.00 | 0.67 | 2.00 | < | < | < |
| | Z2 | 1.50 | 1.23 | < | < | < | < | < | < |
| | Z3 | 2.00 | 2.50 | < | 0.67 | 0.67 | < | < | < |
| | B1 | 2.50 | < | < | < | < | < | < | < |
| | B2 | 1.50 | 2.00 | < | < | < | < | < | < |
| | B3 | 1.00 | 1.50 | < | < | < | < | 0.67 | < |
| Tracheal swab | W1 | 3.50 | 2.67 | 1.00[b] | < | < | < | < | < |
| | W2 | 3.33 | < | < | − | − | − | − | − |
| | W3 | 3.67 | 2.50 | 1.00 | 1.00 | < | 0.67 | < | < |
| | O1 | 3.50 | 3.00 | < | < | < | < | < | < |
| | O2 | 4.50 | 3.67 | 3.00 | < | 0.67 | < | < | < |
| | O3 | 2.50 | 3.67 | 1.50 | < | < | < | < | < |
| | Z1 | 3.00 | 3.33 | 2.33 | 2.00 | 1.23 | < | < | < |
| | Z2 | 1.67 | 2.33 | < | < | < | < | < | < |
| | Z3 | 2.50 | 2.00[b] | 1.50 | < | 0.67 | < | < | < |
| | B1 | 1.50 | < | < | < | < | < | < | < |
| | B2 | 2.33 | 1.23[b] | < | < | < | < | < | < |
| | B3 | 2.77 | 0.67 | < | < | < | < | < | < |
| Bronchial swab | W1 | 2.50 | 0.67 | < | < | < | < | < | < |
| | W2 | 2.67 | 1.00 | < | − | − | − | − | − |
| | W3 | 3.50 | 2.33 | 0.67 | < | < | < | < | < |
| | O1 | 3.00 | 2.67 | 2.00 | < | < | < | < | < |
| | O2 | 2.67 | 2.77 | < | < | < | < | < | < |
| | O3 | 3.67 | 3.33 | 0.67 | < | < | < | < | < |
| | Z1 | 2.50 | 2.23 | 1.50 | < | < | 0.67 | < | < |
| | Z2 | 1.23 | < | 1.00 | < | < | < | < | < |
| | Z3 | 2.33 | 2.50 | < | 0.67 | < | < | < | < |
| | B1 | 2.00 | < | < | < | < | < | < | < |
| | B2 | 3.33 | < | < | < | < | < | < | < |
| | B3 | 2.00 | < | < | < | < | < | < | < |

[a]<, virus titers were below the detection limit (0.67 $log_{10}$ $TCID_{50}$/ml); −, no samples were collected.
[b]Some of the four wells were positive for a cytopathic effect in quadruplicate culture of undiluted samples.

**Severe pneumonia in macaques infected with Dk/HE29-22.** We examined histological inflammation in lung tissues of macaques 8 days after Dk/HE29-22 infection (tissues of animal W2 were collected 3 days after infection.). Although no virus was detected in the lung tissues on day 8 (Table S2), all of the lungs macroscopically showed a dark red color, indicating congestion and inflammation (Fig. S4). The lung of W2 collected on day 3 showed a fresh red color, indicating bleeding near the surface of the lung. The lungs of O2 and O3 also showed a dark red color, indicating bleeding

inside the lungs. The lung lobes of O2 and Z3 were conglutinated with other lung lobes and the thorax. Alveolar spaces were histologically filled with exudate, and average percentages of the affected area in the tissue sections were 71%, 56%, 55%, and 46% in the DW, oseltamivir, zanamivir, and baloxavir groups, respectively. Lymphocytes had infiltrated the alveoli and interstitial areas in all macaques. Bleeding was diffusely seen in the alveoli, especially in the control monkeys (Fig. 2A to J). We evaluated lung inflammation by scoring on the basis of infiltrating immune cells, thickened alveolar walls, bleeding, and exudate (Table S3). The score for W2 lungs was high, indicating severe pneumonia (Fig. 2K). Averages of histological pneumonia in the treated groups showed a tendency to be lower than those in the DW group, although the difference was not statistically significant.

**Cytokine responses in the plasma of macaques infected with Dk/HE29-22 after treatment.** To compare immune responses among the macaques in the four groups, we examined plasma cytokine and chemokine levels (Fig. 3). Levels of interleukin 6 (IL-6) were increased in all groups 1 day after infection. In addition, levels of tumor necrosis factor alpha (TNF-$\alpha$), one of the inflammatory cytokines in addition to IL-6, were slightly increased after virus infection, and the levels of TNF-$\alpha$ in the DW group were higher than those in the other treated groups, although there was no statistical difference. After treatments, levels of interferon alpha (IFN-$\alpha$) in the baloxavir group were higher than those in the other groups on day 3, as were those of IFN-$\beta$ on day 3 and day 5. Levels of monocyte chemotactic protein 1 (MCP-1) in the baloxavir group were the highest of all groups, whereas those in the DW group were low. Levels of IL-13 in the DW group gradually increased, whereas levels of IL-13 in the groups treated with zanamivir and baloxavir decreased after treatments. In the euthanized animal, W2, levels of MIP-1$\alpha$, TNF-$\alpha$, and IL-13 in cerebrospinal fluid (CSF) were higher than those in plasma, indicating that respiratory inflammation affects cytokine responses in the central nervous system (Table S4). Thus, Dk/HE29-22 infection caused vigorous cytokine responses in macaques, and treatment with baloxavir did not inhibit the antiviral cytokine response.

**Increased expression of immune checkpoint molecules on peripheral blood T-lymphocytes of infected macaques.** We investigated the kinetics of expression of immune checkpoint molecules on lymphocytes in peripheral blood (17). During infection, the percentage of $CD4^+$ T cells increased and the percentage of $CD8^+$ T cells slightly decreased in peripheral blood, although there were no significant differences among the groups (data not shown). The percentages of T cells positive for programmed death 1 (PD-1) and T cell immunoreceptor with Ig and ITIM (immunoreceptor tyrosine-based inhibitory motif) domains (TIGIT) in peripheral blood of the euthanized animal, W2, at autopsy were higher than those in the other macaques, although there were no statistically significant differences (Fig. 4; Fig. S5). The percentage of T cells positive for cytotoxic T-lymphocyte-associated antigen 4 (CTLA-4) increased after infection and even after treatment in all groups of macaques. Thus, T cells expressing immune checkpoint molecules increased after infection, indicating that negative feedback regulation of inflammation was induced in all groups.

The distribution of T cells expressing PD-1 in the lung was histologically confirmed. On day 8 after infection, $CD3^+$ T cells had infiltrated into alveoli and bronchus-associated lymphoid tissue (BALT), and some of the $CD3^+$ T cells were positive for PD-1 (Fig. 5A and B). A smaller number of $CD3^+$ T cells were detected in the lung of W2, and no $PD1^+$ $CD3^+$ T cells were detected in the alveoli (Fig. 5C). The percentages of $PD1^+$ cells in $CD3^+$ T cells in the alveoli in the baloxavir group tended to be lower than those in other groups, but the difference was not statistically significant (Fig. 5G). These results suggest that the increase in T cells expressing PD-1 in peripheral blood is followed by infiltration into the local inflammatory area.

## DISCUSSION

In the present study, we characterized the pathogenicity of H7N9 HPAIV Dk/HE29-22 and evaluated the efficacy of a cap-dependent endonuclease inhibitor and NAIs in

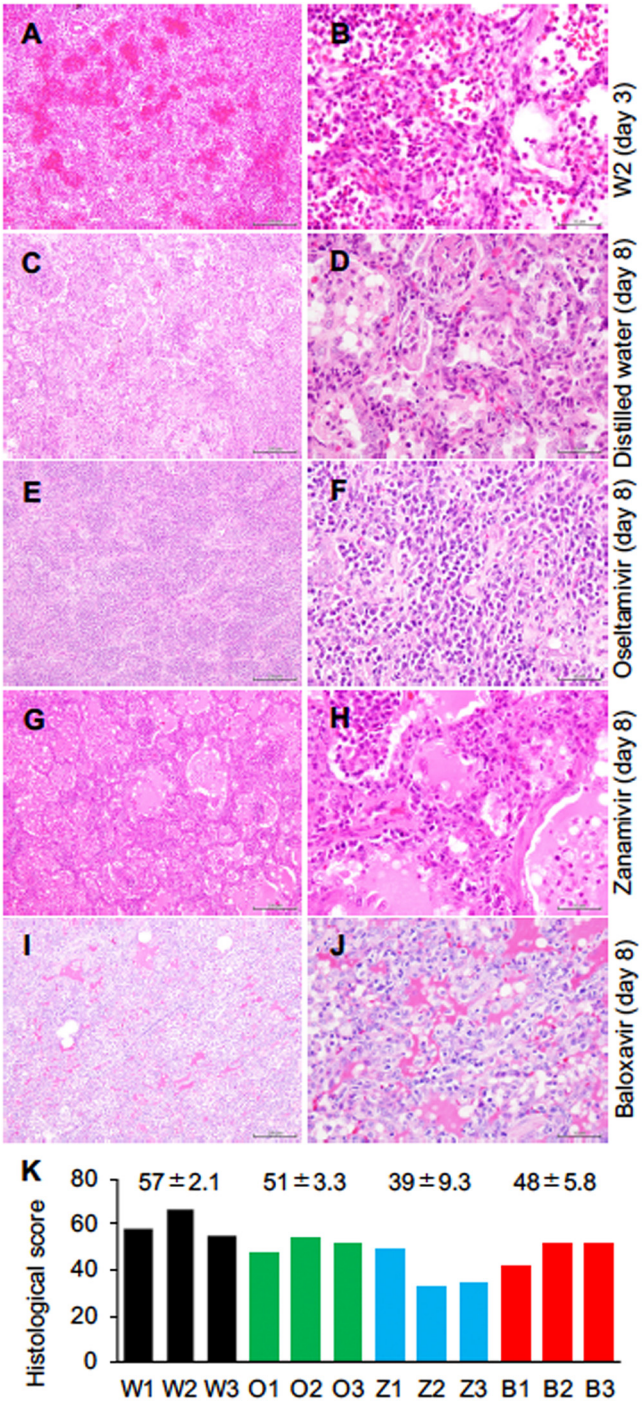


**FIG 2** Viral pneumonia in macaques infected with H7N9 HPAIV. All of the macaques infected with the virus were autopsied 8 days after virus inoculation except for W2, which was autopsied on day 3. Representative photos for each group are shown. (A and B) Lung tissues of a distilled-water control macaque autopsied on day 3 (W2). (C and D) Lung tissues of a distilled-water control macaque autopsied on day 8 (W3). (E and F) Lung tissues of a macaque treated with oseltamivir (O2) that was autopsied on day 8. (G and H) Lung tissues of a macaque treated with zanamivir (Z2) that was autopsied on day 8. (I and J) Lung tissues of a macaque treated with baloxavir (B1) that was autopsied on day 8. Bars, 200 $\mu$m (A, C, E, G, and I) and 50 $\mu$m (B, D, F, H, and J). (K) Summation of histological scores in the six lung lobes of each macaque. Histological scores were determined according to Table S3. Black, DW group; green, oseltamivir group; blue, zanamivir group; and red, baloxavir group. Numbers above the bars are averages and standard deviations for two macaques (DW group; W2 was autopsied on day 3) or three macaques (oseltamivir, zanamivir, and baloxavir groups). No statistically significant differences were found among the groups ($P > 0.05$; Mann-Whitney $U$ test).

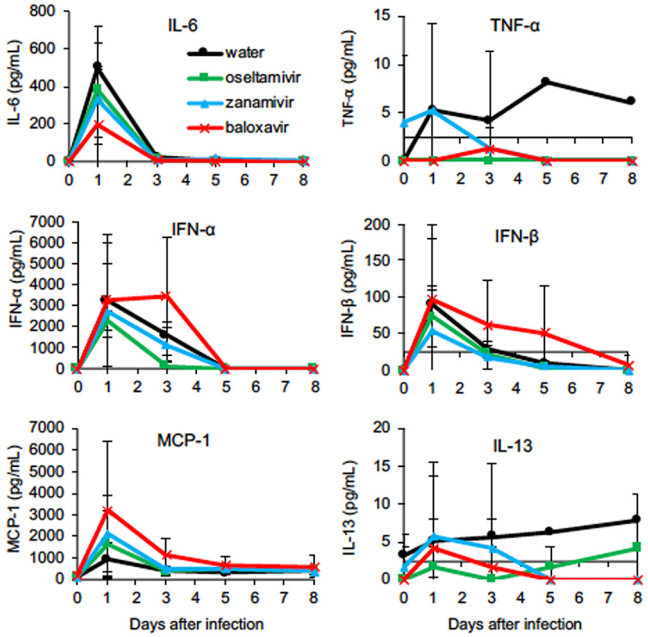


**FIG 3** Levels of cytokines and chemokines in plasma of macaques infected with H7N9 HPAIV. The concentrations of cytokines and chemokines in plasma collected from Dk/HE29-22-infected cynomolgus macaques are shown. Plasma was collected 0, 1, 3, 5, and 8 days after virus inoculation. Averages and standard deviations for three monkeys in each group are shown, except that those in the DW group 4 to 8 days after virus inoculation are for two monkeys. There were no significant differences among the groups ($P > 0.05$; Mann-Whitney *U* test). The *y* values at crossing points at *x* axes indicate detection limits.

cynomolgus macaques. Dk/HE29-22 caused very severe clinical signs of disease in the cynomolgus macaques. Body temperature after infection increased in all groups, and the temperature in the control group did not decrease until the end of this study, whereas the body temperature in the oseltamivir group decreased early. Dk/HE29-22 caused severe pneumonia in macaques, although the virus was mostly eliminated by day 8 in the tissues of all groups. Notably, the virus titers of bronchial swab samples in the baloxavir group were significantly lower than those of swab samples in the macaques of NAI groups, although the number of animals available in the present study was limited. In addition, levels of IFN-$\alpha$ and IFN-$\beta$ in plasma were slightly higher in the baloxavir group after treatment.

One of the three untreated macaques showed lethal clinical signs of disease after Dk/HE29-22 infection. In the euthanized macaque (W2), levels of cytokines in plasma and CSF were extremely high, suggesting systemic inflammatory response syndrome. Although brain edema was not confirmed histologically, the possibility of encephalopathy could not be ruled out. Since the lung of macaque W2 showed severe hemorrhage and lymphocyte infiltration, the major cause of death in macaque W2 is thought to be respiratory failure due to severe viral pneumonia. Severe clinical signs of disease in Dk/HE29-22 infection may be due to 3 and 13 differences in amino acids of the PB1 and PB2 proteins, respectively, from A/Guangdong/17SF003/2016 (H7N9), which showed moderate pathogenicity in macaques in a previous study (13).

Propagation of Dk/HE29-22 was limited to respiratory tissues of the macaques in the present study, although Dk/HE29-22 has a multibasic cleavage site in the HA protein (NCBI protein ID BBA21752.1), PEVPKRKRTAR/GLF, which is digested by ubiquitous proteinases such as furin (6–12). The amino acid glutamine at position 235 (235Q, corresponding to 226Q in the H3 protein) in the HA protein of Dk/HE29-22 indicates binding to the avian-type receptor (18, 19). However, it has been reported that H7N9 HPAIV with 235Q together with 195V (186 in H3 numbering) had a slightly increased binding capacity for avian- and human-type receptors compared with H7N9 LPAIV (6, 12, 20), being consistent with the results of the present study showing that Dk/HE29-22

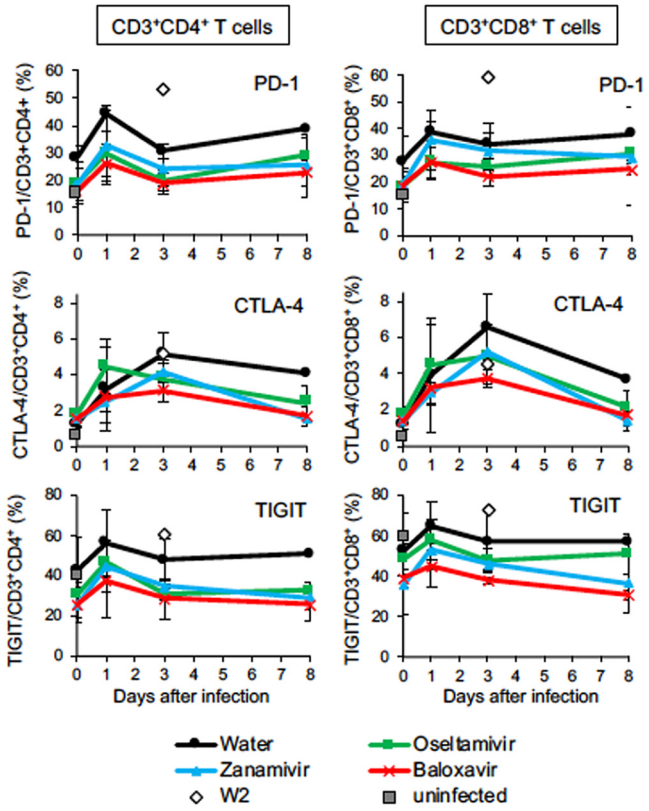


**FIG 4** Percentages of T lymphocytes expressing immune checkpoint molecules during H7N9 HPAIV infection. Peripheral blood mononuclear cells were collected from macaques infected with Dk/HE29-22 virus on days 0, 1, 3, and 8. The percentages of immune checkpoint molecule-positive cells in CD3/CD4-positive cells (left column) and CD3/CD8-positive cells (right column) are shown. Gates for analysis are shown in Fig. S5. Open diamonds, percentages of immune checkpoint molecule-positive cells in W2 at autopsy; gray squares, average percentages of immune checkpoint molecule-positive cells in uninfected macaques ($n = 2$). Averages and standard deviations for the results of three monkeys are shown, except that those in the DW group 4 to 8 days after virus inoculation are for two monkeys. There were no significant differences among the groups ($P > 0.05$; Mann-Whitney *U* test).

proliferated in the upper and lower respiratory tracts of the macaques, of which respiratory epithelial cells are thought to express the human-type receptor in the upper respiratory tract and the avian-type receptor in the lower respiratory tract (21, 22).

We previously found a mutation at position 235Q in the HA from NAI-resistant H7N9 LPAIV (NA289K/HA235Q) (14, 23). However, the NAI-resistant mutation 289K (R292K in reference 24) was not detected in the inoculum virus of Dk/HE29-22 (6). Furthermore, reduction in replication of LPAIV and HPAIV caused by oseltamivir in a previous *in vitro* study was comparable to that caused by baloxavir (15). However, in the present study, oseltamivir and zanamivir did not show significant effects on virus titers. Therefore, further studies are required to determine the reason for the different effects of NAIs against HPAIV. On the other hand, baloxavir acid, which is the active form of baloxavir marboxil, exhibited comparable potencies against LPAIV and HPAIV, including LPAIV with an NAI-resistant variant (15). *In vivo* studies using mice showed that baloxavir inhibited propagation of H7N9 HPAIV more effectively than did oseltamivir (15, 16), which is in agreement with the results of the present study for macaques infected with H7N9 HPAIV.

Inflammatory cytokines were produced in macaques infected with Dk/HE29-22. Levels of IL-6 and MCP-1 were increased dramatically 1 day after infection, and then the levels decreased within a few days in macaques of all groups. In the baloxavir group, high levels of type I IFN, including IFN-$\alpha$ and IFN-$\beta$, lasted longer than those in

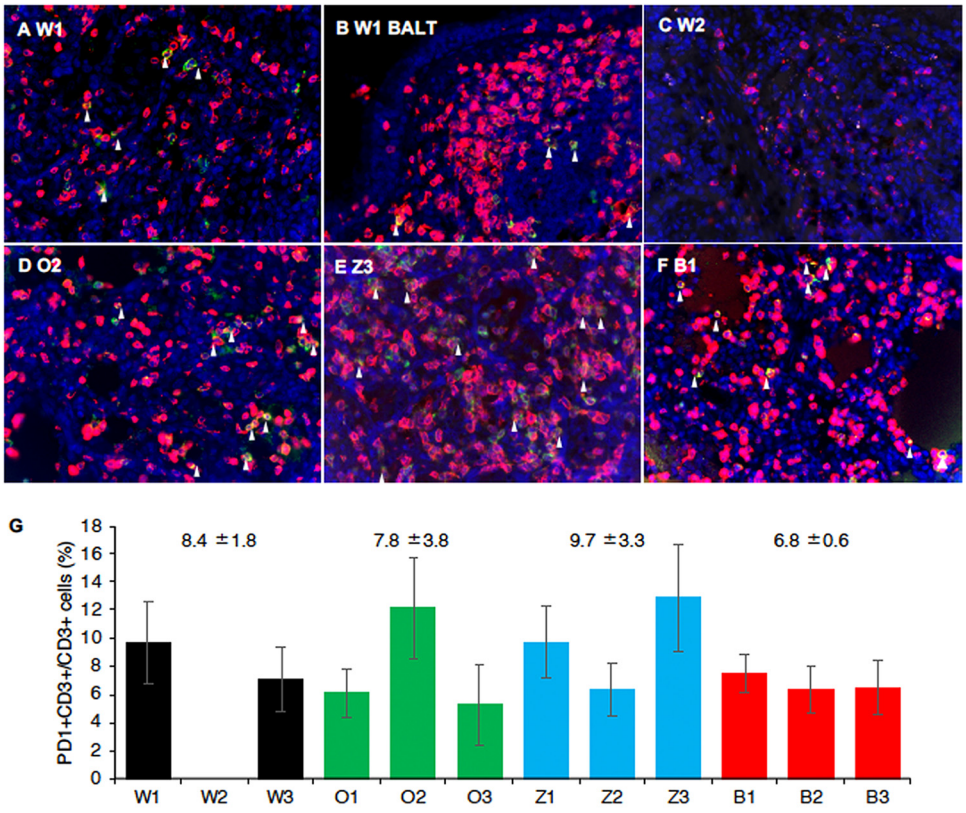


**FIG 5** Infiltration of PD1$^+$ CD3$^+$ T lymphocytes in the lungs of macaques after H7N9 HPAIV infection. (A to F) PD-1 and CD3 were stained on lung tissue sections. (A and C to F) Lung parenchyma; (B) BALT. (A and B) W1, autopsied on day 8; (C) W2, autopsied on day 3; (D) O2; (E) Z3; (F) B1, autopsied on day 8. Green, PD1; red, CD3; blue, nuclei (DAPI) imaged with a 40 × lens objective. White arrowheads show representative PD-1$^+$ CD3$^+$ cells. (G) PD-1$^+$ CD3$^+$ cells in lung tissues of each macaque. Black, DW group; green, oseltamivir group; blue, zanamivir group; and red, baloxavir group. Averages and standard deviations of the percentages of PD-1$^+$ CD3$^+$ cells in 5 images of lung parenchyma tissue sections in individual macaques are shown. Numbers above the bars are averages and standard deviations for two macaques (DW group; W2 was autopsied on day 3) or three macaques (oseltamivir, zanamivir, and baloxavir groups). No statistically significant differences were found among the groups ($P > 0.05$; Mann-Whitney *U* test).

other groups, suggesting that low virus titers in the baloxavir group prevent suppression of host innate immune responses by viral proteins such as NS gene products (25) and that the persistence of type I IFN at high levels might have contributed to inhibition of virus propagation in addition to a direct inhibitory effect of baloxavir. Furthermore, type I IFN has been shown to facilitate maturation of dendritic cells and to promote activation of lymphocytes (26–28). On the other hand, the levels of IL-6 and TNF-$\alpha$ were low or under the detection limit in the baloxavir group. Since the virus titer in the baloxavir group was the lowest among the groups, it is thought that the high titer of Dk/HE29-22 except for that in the baloxavir group induced a potent inflammatory reaction. Only in the DW group, the level of IL-13 increased until day 8, suggesting the involvement of IL-13 in pneumonia and lung tissue repair (29–33), which is consistent with histological findings.

A transient increase in the percentage of T cells positive for immune checkpoint molecules was seen in peripheral blood 1 day after infection, followed by infiltration of the T cells into lung tissues. Levels of PD-1 and CTLA-4 expression on the surfaces of CD4$^+$ and CD8$^+$ T cells in peripheral blood increased in macaques in the DW group, which had more severe pneumonia than macaques in the other groups. Since virus antigen-specific T cells were not identified in the present study, T cells expressing the immune checkpoint molecules might be not only specific but also nonspecific for virus antigens, including bystander activation, especially at early time points such as days 1

and 3. The percentage of PD-1$^+$ T cells in peripheral blood in animal W2 on day 3 was the highest of all macaques, whereas the percentages of CD4$^+$ and CD8$^+$ T cells positive for PD-1, CTLA-4, and TIGIT in the baloxavir group tended to be lower than those in the other groups. Since PD-1$^+$ T cells were not observed in the lung of W2 (Fig. 5G), this subpopulation is thought to have been activated outside the lung on day 3 and to have been recruited to the inflammatory site by day 8. These molecules are known to selectively regulate the effector function of CD8$^+$ T cells in acute and chronic virus infections (34–36). Therefore, in Dk/HE29-22 infection, negative feedback responses on T cells were induced after activation of acute inflammatory responses. Hence, the high expression levels of PD-1 and TIGIT in W2 suggest that the high pathogenicity of Dk/HE29-22 is partly due to potent negative feedback and suppression of T cell responses, which may inhibit viral clearance at an early stage of infection.

All of the macaques infected with Dk/HE29-22 showed severe clinical signs of disease, and one of the three control macaques reached a humane endpoint 3 days after infection. The results indicate that the H7N9 HPAIV strain might be pathogenic in humans. Although baloxavir inhibited virus propagation, resulting in prevention of excessive immune responses, lung damage was apparent in treated macaques. Active surveillance of H7N9 HPAIV/LPAIV in poultry and imported products is required to prevent spread of the virus.

## MATERIALS AND METHODS

**Ethics statement.** This study was carried out in strict accordance with the Guidelines for the Husbandry and Management of Laboratory Animals of the Research Center for Animal Life Science at Shiga University of Medical Science and Standards Relating to the Care and Fundamental Guidelines for Proper Conduct of Animal Experiments and Related Activities in Academic Research Institutions under the jurisdiction of the Ministry of Education, Culture, Sports, Science and Technology of Japan. The protocols were approved by the Shiga University of Medical Science Animal Experiment Committee (permit number 2018-5-10 [H1]). The Research Center for Animal Life Science at Shiga University of Medical Science has a permit for importation of cynomolgus macaques. Regular veterinary care and monitoring, balanced nutrition, and environmental enrichment were provided by the Research Center for Animal Life Science at Shiga University of Medical Science. The macaques were euthanized at the endpoint of 8 days after virus inoculation using ketamine (5 mg/kg of body weight; Daiichi Sankyo Propharma, Co., Ltd., Tokyo, Japan) and xylazine (1 mg/kg; Bayer, Ltd., Osaka, Japan) followed by an injection of sodium pentobarbital (200 mg/kg of body weight; Kyoritsu Seiyaku, Corp., Tokyo, Japan). The animals were monitored every day during the study to be clinically scored as described in Table S1 (37) and to undergo veterinary examinations to help alleviate suffering. Animals were scheduled to be euthanized if their clinical scores reached 15 (a humane endpoint).

**Animals.** Female cynomolgus macaques (4 to 5 years of age) bred from macaques originating in China in the Research Center for Animal Life Science, Shiga University of Medical Science, were used. The cynomolgus macaques used in the present study were healthy young adults. Sample collection and virus inoculation were performed under conditions of ketamine (5 mg/kg) and xylazine (1 mg/kg) anesthesia, and all efforts were made to minimize suffering. CMK-2 food pellets (CLEA Japan, Inc., Tokyo, Japan) were given once a day after recovery from anesthesia, and drinking water was available *ad libitum*. The animals were individually housed under conditions of controlled humidity (47% to 54%), temperature (23 to 24°C), and light (12-h light/12-h dark cycle; lights on at 8:00 a.m.). In the text and figures, individual macaques are distinguished by the following identification numbers: W1, W2, and W3 are macaques without treatment; O1, O2, and O3 are macaques treated with oseltamivir; Z1, Z2, and Z3 are macaques treated with zanamivir; and B1, B2, and B3 are macaques treated with baloxavir.

Two weeks before virus inoculation, a telemetry probe (TA10CTA-D70; Data Sciences International, St. Paul, MN) was implanted in the peritoneal cavity of each macaque under conditions of ketamine/xylazine anesthesia followed by isoflurane (Zoetis JP, Inc., Tokyo, Japan) inhalation to monitor vital signs. The macaques used in the present study were free from herpes B virus, hepatitis E virus, *Mycobacterium tuberculosis*, *Shigella* spp., *Salmonella* spp., and *Entamoeba histolytica*. Under conditions of ketamine/xylazine anesthesia, two cotton sticks were used to collect fluid samples in eyes, nasal cavities, oral cavities, and tracheas every day from day 0 to day 8, and the sticks were subsequently immersed in 1 ml of Eagle's minimal essential medium (EMEM; Nacalai Tesque) containing 0.1% bovine serum albumin (BSA) and antibiotics. A bronchoscope (MEV-2560; Machida Endoscope Co. Ltd., Tokyo, Japan) and cytology brushes (BC-203D-2006; Olympus Co., Tokyo, Japan) were used to obtain bronchial samples (38).

**Viruses and cells.** The challenge virus strain A/duck/Japan/AQ-HE29-22/2017 (H7N9) (Dk/HE29-22) (NCBI taxonomy ID 2027165) was isolated from a Muscovy duck (*Cairina moschata*) meat product using embryonated chicken eggs (6) following propagation in 10-day-old embryonated chicken eggs (obtained from Sasaki Chemical, Co. Ltd., Kyoto, Japan) at 35°C for 1 day. Propagated virus was titrated by 50% tissue culture infective doses ($TCID_{50}$)/ml. For virus titration, briefly, serial dilutions of swabs or tissue homogenate samples were inoculated onto confluent Madin-Darby canine kidney (MDCK) cells (American Type Culture Collection, Manassas, VA) (39). The MDCK cells were then cultured in EMEM

including 0.1% BSA and penicillin/streptomycin. The presence of cytopathic effects was determined under a microscope 72 h later, and virus titers were calculated.

Twelve macaques ($n = 3$ in each group) were challenged with Dk/HE29-22 ($3 \times 10^6$ $TCID_{50}$ in 7 ml Hanks buffered saline solution). The virus was inoculated into conjunctivas (0.05 ml for each conjunctiva), nostrils (0.5 ml for each nostril), oral cavities (0.9 ml), and tracheas (5 ml) with pipettes and catheters. Experiments using the challenge virus were performed in the biosafety level 3 facility of the Research Center for Animal Life Science, Shiga University of Medical Science.

**Compounds.** Oseltamivir phosphate (Chugai Pharmaceutical Co., Ltd., Tokyo, Japan), zanamivir hydrate (GlaxoSmithKline plc., London, Britain), baloxavir marboxil (Shionogi & Co., Ltd., Osaka, Japan), and distilled water (Otsuka Pharmaceutical Co., Ltd., Tokyo, Japan) were purchased from Masuda Medical Instruments, Kyoto, Japan. Oseltamivir phosphate (3% concentration in dry syrup) was dissolved in water at 30 mg oseltamivir phosphate/2 ml and administered in the stomach with catheters (30 mg/2 ml/kg of body weight/day) once a day from day 1 to day 5 after infection, which provided a higher blood concentration of oseltamivir carboxylate than did a human adult dose (75 mg) (40). Zanamivir hydrate was dissolved in saline at 10 mg/ml and administered in the trachea with a vaporizer (10 mg/ml/animal/day) once a day from day 1 to day 5 after infection. A baloxavir marboxil capsule was crushed and dissolved in distilled water at 1 mg/2 ml and administered in the stomach with catheters (1 mg/2 ml/kg of body weight/day) once on day 1 after infection. For the control group, distilled water was administered in the stomach (2 ml/kg of body weight/day) and phosphate-buffered saline (PBS, 1 ml/animal/day) was administered in the trachea, being equivalent to drug administrations in other groups, once a day from day 1 to day 5 after infection.

**Histopathological examination and staining.** Lung tissues obtained at autopsy were immersed in 10% neutral buffered formalin, embedded in paraffin, and cut into 3-$\mu$m-thick sections. The sections were stained with hematoxylin and eosin (H&E).

**Multiplex cytokine detection assay.** Peripheral blood of all macaques was collected on days 0, 1, 3, 5, 7, and 8 after virus inoculation. The concentrations of cytokines and chemokines (IL-6, IL-13, TNF-$\alpha$, and MCP-1) were determined using a Milliplex bead array assay (Merck Millipore, Billerica, MA) according to the manufacturer's instructions. The samples were analyzed using the Luminex 200 system (Merck Millipore). Concentrations of IFN-$\alpha$ and IFN-$\beta$ were determined using a Verkine cynomolgus/rhesus interferon alpha serum enzyme-linked immunosorbent assay (ELISA) kit (PBL Assay Science, Piscataway, NJ) and a Verkine-HS human interferon beta serum ELISA kit (PBL Assay Science) according to the manufacturer's instructions. The samples were analyzed using the GloMax Explorer system (Promega Corporation, Madison, WI).

**Flow cytometry.** Peripheral blood mononuclear cells (PBMCs) were isolated from heparinized whole blood using LeucoSep (Greiner Bio-One, Kremsmuenster, Austria) and were stored in Cellbanker (Nippon Zenyaku Kogyo Co., Ltd., Koriyama, Japan) at −80°C until use. Frozen PBMCs were thawed in a 37°C water bath and incubated for 10 min with FcR blocking reagent (Miltenyi Biotec, Bergisch Gladbach, Germany), and then dead cells were stained with Zombie Aqua (BioLegend, Inc., San Diego, CA) for 20 min. For surface staining, we used antibodies against the following molecules: CD3-allophycocyanin (APC)-Cy7 (BD Biosciences, Franklin Lakes, NJ), CD4-fluorescein isothiocyanate (FITC) (BioLegend), CD8-phycoerythrin (PE)-Cy7 (BD Biosciences), CD25-APC (eBioscience, Waltham, MA), CD20-PE-Cy5 (BD Biosciences), CTLA-4-BV421 (BD), PD-1-BV421 (BioLegend), and TIGIT-PE (eBioscience). We used mouse or rat IgG isotype antibodies for each as an isotype control. After incubation for 30 min, cells were washed twice and fixed in 4% paraformaldehyde–PBS. After being washed twice, samples were analyzed using CytoFLEX (Beckman Coulter, Inc., Brea, CA).

**Immunofluorescence staining of tissue sections.** Three-micrometer-thick formalin-fixed paraffin-embedded tissue sections were deparaffinized by a standard method with xylene and ethanol, and then endogenous peroxidase activity was blocked with methanol containing 1% hydrogen peroxidase for 13 min. Antigens were retrieved at 121°C for 1 min in pH 7.0 citrate buffer. Next, nonspecific antibody binding was blocked with goat serum for 30 min, and anti-PD-1 antibody (Abcam no. Ab52587; 1:100 dilution) was added. After overnight incubation, the sections were incubated with horseradish peroxidase (HRP)-conjugated secondary antibody (Simple Stain MAX-PO [MULTI]; Nichirei Bioscience) for 60 min and treated with tyramide signal amplification (TSA) plus fluorescence (OPAL520 fluorophore, 1:50 dilution, Perkin Elmer Life and Analytical Sciences, Boston, MA) for 10 min. After being washed, the sections were stained with anti-CD3 antibody (Dako no. M7254; 1:500 dilution) overnight and then incubated with HRP-conjugated secondary antibody for 60 min. Tissues were treated with TSA plus cyanin 3 (OPAL570 fluorophore, 1:100 dilution; Perkin Elmer Life and Analytical Sciences) for 10 min. Next, autofluorescence was removed by a Vector TrueVIEW autofluorescence quenching kit following the manufacturer's instructions. Lastly, sections were counterstained and mounted with Prolong Gold antifade reagent with DAPI (4′,6-diamidino-2-phenylindole; Invitrogen no. P36935) and then observed under a microscope (BX-X710; Keyence, Osaka, Japan). As a control, a tissue section was stained with mouse IgG1 isotype control (Dako no. X0931).

**Statistical analysis.** Statistical significance between groups was determined using the Mann-Whitney *U* test.

## SUPPLEMENTAL MATERIAL

Supplemental material is available online only.

**SUPPLEMENTAL FILE 1**, PDF file, 1.1 MB.

## ACKNOWLEDGMENTS

This work was supported by a grant from the Ministry of Education, Culture, Sports, Science and Technology, Japan, for a Joint Research Program of the Research Center for Zoonosis Control, Hokkaido University, and the Japan Initiative for Global Research Network on Infectious Diseases (J-GRID) of the Japan Agency for Medical Research and Development (AMED) under grant number JP19fm0108008, JSPS KAKENHI grant numbers 18K15117 and 15H04720, and by a grant from President's research grant in Shiga University of Medical Science. Cong Thanh Nguyen is supported by the Sato Yo International Scholarship Foundation. The funders had no role in study design, data collection and interpretation, or the decision to submit the work for publication.

We thank Hideaki Tsuchiya, Takahiro Nakagawa, Ikuo Kawamoto, and Iori Itagaki for animal care and Naoko Kitagawa, Hideaki Ishida, and Takako Sasamura for helping with animal experiments.

## REFERENCES

1. Gao R, Cao B, Hu Y, Feng Z, Wang D, Hu W, Chen J, Jie Z, Qiu H, Xu K, Xu X, Lu H, Zhu W, Gao Z, Xiang N, Shen Y, He Z, Gu Y, Zhang Z, Yang Y, Zhao X, Zhou L, Li X, Zou S, Zhang Y, Li X, Yang L, Guo J, Dong J, Li Q, Dong L, Zhu Y, Bai T, Wang S, Hao P, Yang W, Zhang Y, Han J, Yu H, Li D, Gao GF, Wu G, Wang Y, Yuan Z, Shu Y. 2013. Human infection with a novel avian-origin influenza A (H7N9) virus. N Engl J Med 368:1888–1897. https://doi.org/10.1056/NEJMoa1304459.
2. World Health Organization (WHO). 2020. Influenza at the human-animal interface, summary and assessment, from 11 July to 23 October 2020.
3. OIE. 2017. Immediate notification report. Report OIE 22933, People's Republic of China.
4. Qi W, Jia W, Liu D, Li J, Bi Y, Xie S, Li B, Hu T, Du Y, Xing L, Zhang J, Zhang F, Wei X, Eden JS, Li H, Tian H, Li W, Su G, Lao G, Xu C, Xu B, Liu W, Zhang G, Ren T, Holmes EC, Cui J, Shi W, Gao GF, Liao M. 2017. Emergence and adaptation of a novel highly pathogenic H7N9 influenza virus in birds and humans from a 2013 human-infecting low-pathogenic ancestor. J Virol 92:e00921-17. https://doi.org/10.1128/JVI.00921-17.
5. Su S, Gu M, Liu D, Cui J, Gao GF, Zhou J, Liu X. 2017. Epidemiology, evolution, and pathogenesis of H7N9 influenza viruses in five epidemic waves since 2013 in China. Trends Microbiol 25:713–728. https://doi.org/10.1016/j.tim.2017.06.008.
6. Shibata A, Okamatsu M, Sumiyoshi R, Matsuno K, Wang ZJ, Kida H, Osaka H, Sakoda Y. 2018. Repeated detection of H7N9 avian influenza viruses in raw poultry meat illegally brought to Japan by international flight passengers. Virology 524:10–17. https://doi.org/10.1016/j.virol.2018.08.001.
7. Wu L, Mitake H, Kiso M, Ito M, Iwatsuki-Hirimoto K, Yamayoshi S, Lopes TJS, Feng H, Sumiyoshi R, Shibata A, Osaka H, Imai M, Watanabe T, Kawaoka Y. 2020. Characterization of H7N9 avian influenza viruses isolated from duck meat products. Transbound Emerg Dis 67:792–798. https://doi.org/10.1111/tbed.13398.
8. OIE. 2017. Infection with avian influenza viruses. Terrestrial animal health code, chapter 10.4. World Organisation for Animal Health, Paris, France. https://www.oie.int/fileadmin/Home/eng/Health_standards/tahc/current/chapitre_avian_influenza_viruses.pdf.
9. Ke C, Mok CKP, Zhu W, Zhou H, He J, Guan W, Wu J, Song W, Wang D, Liu J, Lin Q, Chu DKW, Yang L, Zhong N, Yang Z, Shu Y, Peiris JSM. 2017. Human infection with highly pathogenic avian influenza A(H7N9) virus, China. Emerg Infect Dis 23:1332–1340. https://doi.org/10.3201/eid2308.170600.
10. Quan C, Shi W, Yang Y, Yang Y, Liu X, Xu W, Li H, Li J, Wang Q, Tong Z, Wong G, Zhang C, Ma S, Ma Z, Fu G, Zhang Z, Huang Y, Song H, Yang L, Liu WJ, Liu Y, Liu W, Gao GF, Bi Y. 2018. New threats from H7N9 influenza virus: spread and evolution of high- and low-pathogenicity variants with high genomic diversity in wave five. J Virol 92:e00301-18. https://doi.org/10.1128/JVI.00301-18.
11. de Vries RP, Peng W, Grant OC, Thompson AJ, Zhu X, Bouwman KM, de la Pena ATT, van Breemen MJ, Ambepitiya Wickramasinghe IN, de Haan CAM, Yu W, McBride R, Sanders RW, Woods RJ, Verheije MH, Wilson IA, Paulson JC. 2017. Three mutations switch H7N9 influenza to human-type receptor specificity. PLoS Pathog 13:e1006390. https://doi.org/10.1371/journal.ppat.1006390.
12. Xu Y, Peng R, Zhang W, Qi J, Song H, Liu S, Wang H, Wang M, Xiao H, Fu L, Fan Z, Bi Y, Yan J, Shi Y, Gao GF. 2019. Avian-to-human receptor-binding adaptation of avian H7N9 influenza virus hemagglutinin. Cell Rep 29:2217–2228.E5. https://doi.org/10.1016/j.celrep.2019.10.047.
13. Imai M, Watanabe T, Kiso M, Nakajima N, Yamayoshi S, Iwatsuki-Horimoto K, Hatta M, Yamada S, Ito M, Sakai-Tagawa Y, Shirakura M, Takashita E, Fujisaki S, McBride R, Thompson AJ, Takahashi K, Maemura T, Mitake H, Chiba S, Zhong G, Fan S, Oishi K, Yasuhara A, Takada K, Nakao T, Fukuyama S, Yamashita M, Lopes TJS, Neumann G, Odagiri T, Watanabe S, Shu Y, Paulson JC, Hasegawa H, Kawaoka Y. 2017. A highly pathogenic avian H7N9 influenza virus isolated from a human is lethal in some ferrets infected via respiratory droplets. Cell Host Microbe 22:615–626.E8. https://doi.org/10.1016/j.chom.2017.09.008.
14. Itoh Y, Shichinohe S, Nakayama M, Igarashi M, Ishii A, Ishigaki H, Ishida H, Kitagawa N, Sasamura T, Shiohara M, Doi M, Tsuchiya H, Nakamura S, Okamatsu M, Sakoda Y, Kida H, Ogasawara K. 2015. Emergence of H7N9 influenza A virus resistant to neuraminidase inhibitors in nonhuman primates. Antimicrob Agents Chemother 59:4962–4973. https://doi.org/10.1128/AAC.00793-15.
15. Taniguchi K, Ando Y, Nobori H, Toba S, Noshi T, Kobayashi M, Kawai M, Yoshida R, Sato A, Shishido T, Naito A, Matsuno K, Okamatsu M, Sakoda Y, Kida H. 2019. Inhibition of avian-origin influenza A(H7N9) virus by the novel cap-dependent endonuclease inhibitor baloxavir marboxil. Sci Rep 9:3466. https://doi.org/10.1038/s41598-019-39683-4.
16. Kiso M, Yamayoshi S, Furusawa Y, Imai M, Kawaoka Y. 2019. Treatment of highly pathogenic H7N9 virus-infected mice with baloxavir marboxil. Viruses 11:1066. https://doi.org/10.3390/v11111066.
17. Anderson AC, Joller N, Kuchroo VK. 2016. Lag-3, Tim-3, and TIGIT: co-inhibitory receptors with specialized functions in immune regulation. Immunity 44:989–1004. https://doi.org/10.1016/j.immuni.2016.05.001.
18. Shichinohe S, Okamatsu M, Sakoda Y, Kida H. 2013. Selection of H3 avian influenza viruses with SA$\alpha$2,6Gal receptor specificity in pigs. Virology 444:404–408. https://doi.org/10.1016/j.virol.2013.07.007.
19. Rogers GN, Paulson JC, Daniels RS, Skehel JJ, Wilson IA, Wiley DC. 1983. Single amino acid substitutions in influenza haemagglutinin change receptor binding specificity. Nature 304:76–78. https://doi.org/10.1038/304076a0.
20. Zhu W, Zhou J, Li Z, Yang L, Li X, Huang W, Zou S, Chen W, Wei H, Tang J, Liu L, Dong J, Wang D, Shu Y. 2017. Biological characterisation of the emerged highly pathogenic avian influenza (HPAI) A(H7N9) viruses in humans, in mainland China, 2016 to 2017. Euro Surveill 22:30533. https://doi.org/10.2807/1560-7917.ES.2017.22.19.30533.
21. van Riel D, Munster VJ, de Wit E, Rimmelzwaan GF, Fouchier RA, Osterhaus AD, Kuiken T. 2006. H5N1 virus attachment to lower respiratory tract. Science 312:399. https://doi.org/10.1126/science.1125548.
22. Watanabe T, Kiso M, Fukuyama S, Nakajima N, Imai M, Yamada S, Murakami S, Yamayoshi S, Iwatsuki-Horimoto K, Sakoda Y, Takashita E, McBride R, Noda T, Hatta M, Imai H, Zhao D, Kishida N, Shirakura M, de Vries RP, Shichinohe S, Okamatsu M, Tamura T, Tomita Y, Fujimoto N, Goto K, Katsura H, Kawakami E, Ishikawa I, Watanabe S, Ito M, Sakai-Tagawa Y, Sugita Y, Uraki R, Yamaji R, Eisfeld AJ, Zhong G, Fan S, Ping J, Maher EA, Hanson A, Uchida Y, Saito T, Ozawa M, Neumann G, Kida H, Odagiri T, Paulson JC, Hasegawa H, Tashiro M, Kawaoka Y. 2013.

Characterization of H7N9 influenza A viruses isolated from humans. Nature 501:551–555. https://doi.org/10.1038/nature12392.
23. Suzuki S, Shichinohe S, Itoh Y, Nakayama M, Ishigaki H, Mori Y, Ogata-Nakahara A, Nguyen CT, Okamatsu M, Sakoda Y, Kida H, Ogasawara K. 2020. Low replicative fitness of neuraminidase inhibitor-resistant H7N9 avian influenza A virus with R292K substitution in neuraminidase in cynomolgus macaques compared with I222T substitution. Antiviral Res 178:104790. https://doi.org/10.1016/j.antiviral.2020.104790.
24. Zhang F, Bi Y, Wang J, Wong G, Shi W, Hu F, Yang Y, Yang L, Deng X, Jiang S, He X, Liu Y, Yin C, Zhong N, Gao GF. 2017. Human infections with recently-emerging highly pathogenic H7N9 avian influenza virus in China. J Infect 75:71–75. https://doi.org/10.1016/j.jinf.2017.04.001.
25. García-Sastre A, Egorov A, Matassov D, Brandt S, Levy DE, Durbin JE, Palese P, Muster T. 1998. Influenza A virus lacking the NS1 gene replicates in interferon-deficient systems. Virology 252:324–330. https://doi.org/10.1006/viro.1998.9508.
26. Tough DF, Borrow P, Sprent J. 1996. Induction of bystander T cell proliferation by viruses and type I interferon in vivo. Science 272:1947–1950. https://doi.org/10.1126/science.272.5270.1947.
27. Marrack P, Kappler J, Mitchell T. 1999. Type I interferons keep activated T cells alive. J Exp Med 189:521–530. https://doi.org/10.1084/jem.189.3.521.
28. Cella M, Salio M, Sakakibara Y, Langen H, Julkunen I, Lanzavecchia A. 1999. Maturation, activation, and protection of dendritic cells induced by double-stranded RNA. J Exp Med 189:821–829. https://doi.org/10.1084/jem.189.5.821.
29. Zhu Z, Ma B, Zheng T, Homer RJ, Lee CG, Charo IF, Noble P, Elias JA. 2002. IL-13-induced chemokine responses in the lung: role of CCR2 in the pathogenesis of IL-13-induced inflammation and remodeling. J Immunol 168:2953–2962. https://doi.org/10.4049/jimmunol.168.6.2953.
30. Price GE, Gaszewska-Mastarlarz A, Moskophidis D. 2000. The role of alpha/beta and gamma interferons in development of immunity to influenza A virus in mice. J Virol 74:3996–4003. https://doi.org/10.1128/jvi.74.9.3996-4003.2000.
31. Cohn L, Tepper JS, Bottomly K. 1998. IL-4-independent induction of airway hyperresponsiveness by Th2, but not Th1, cells. J Immunol 161:3813–3816.
32. Cohn L, Homer RJ, Marinov A, Rankin J, Bottomly K. 1997. Induction of airway mucus production By T helper 2 (Th2) cells: a critical role for interleukin 4 in cell recruitment but not mucus production. J Exp Med 186:1737–1747. https://doi.org/10.1084/jem.186.10.1737.
33. Kibe A, Inoue H, Fukuyama S, Machida K, Matsumoto K, Koto H, Ikegami T, Aizawa H, Hara N. 2003. Differential regulation by glucocorticoid of interleukin-13-induced eosinophilia, hyperresponsiveness, and goblet cell hyperplasia in mouse airways. Am J Respir Crit Care Med 167:50–56. https://doi.org/10.1164/rccm.2110084.
34. Johnston RJ, Comps-Agrar L, Hackney J, Yu X, Huseni M, Yang Y, Park S, Javinal V, Chiu H, Irving B, Eaton DL, Grogan JL. 2014. The immunoreceptor TIGIT regulates antitumor and antiviral $CD8^+$ T cell effector function. Cancer Cell 26:923–937. https://doi.org/10.1016/j.ccell.2014.10.018.
35. Rutigliano JA, Sharma S, Morris MY, Oguin TH, 3rd, McClaren JL, Doherty PC, Thomas PG. 2014. Highly pathological influenza A virus infection is associated with augmented expression of PD-1 by functionally compromised virus-specific $CD8^+$ T cells. J Virol 88:1636–1651. https://doi.org/10.1128/JVI.02851-13.
36. Yu X, Harden K, Gonzalez LC, Francesco M, Chiang E, Irving B, Tom I, Ivelja S, Refino CJ, Clark H, Eaton D, Grogan JL. 2009. The surface protein TIGIT suppresses T cell activation by promoting the generation of mature immunoregulatory dendritic cells. Nat Immunol 10:48–57. https://doi.org/10.1038/ni.1674.
37. Pham VL, Nakayama M, Itoh Y, Ishigaki H, Kitano M, Arikata M, Ishida H, Kitagawa N, Shichinohe S, Okamatsu M, Sakoda Y, Tsuchiya H, Nakamura S, Kida H, Ogasawara K. 2013. Pathogenicity of pandemic H1N1 influenza A virus in immunocompromised cynomolgus macaques. PLoS One 8:e75910. https://doi.org/10.1371/journal.pone.0075910.
38. Nakayama M, Shichinohe S, Itoh Y, Ishigaki H, Kitano M, Arikata M, Pham VL, Ishida H, Kitagawa N, Okamatsu M, Sakoda Y, Ichikawa T, Tsuchiya H, Nakamura S, Le QM, Ito M, Kawaoka Y, Kida H, Ogasawara K. 2013. Protection against H5N1 highly pathogenic avian and pandemic (H1N1) 2009 influenza virus infection in cynomolgus monkeys by an inactivated H5N1 whole particle vaccine. PLoS One 8:e82740. https://doi.org/10.1371/journal.pone.0082740.
39. Itoh Y, Ozaki H, Tsuchiya H, Okamoto K, Torii R, Sakoda Y, Kawaoka Y, Ogasawara K, Kida H. 2008. A vaccine prepared from a non-pathogenic H5N1 avian influenza virus strain confers protective immunity against highly pathogenic avian influenza virus infection in cynomolgus macaques. Vaccine 26:562–572. https://doi.org/10.1016/j.vaccine.2007.11.031.
40. Kitano M, Itoh Y, Kodama M, Ishigaki H, Nakayama M, Ishida H, Baba K, Noda T, Sato K, Nihashi Y, Kanazu T, Yoshida R, Torii R, Sato A, Ogasawara K. 2011. Efficacy of single intravenous injection of peramivir against influenza B virus infection in ferrets and cynomolgus macaques. Antimicrob Agents Chemother 55:4961–4970. https://doi.org/10.1128/AAC.00412-11.